C-19 STATIC AND FATIGUE FRACTURES OF PORTLAND CEMENT MORTAR IN FLEXURE

Joseph Glucklich [1]

ABSTRACT

Experimental work to study the mechanics of fatigue cracks propagation in mortar is presented. Unnotched beams were fatigue loaded with two ranges of stress. Notched beams were similarly loaded with three ranges of stress. The effect of range of stress on the S-N curves was thus partially studied. Stress-strain characteristics during fatigue life were determined. Measured strains were interpreted in terms of crack length, the correlation between compliance and crack length having been pre-determined in static tests. The product of the critical crack length and the square of the maximum stress proved to be a constant number for either unnotched beams or beams with approximately equal notch depths. However, the material constant was found to be G_c, the critical strain-energy release rate, as it had almost the same numerical value for both notched and unnotched beams. Comparing G_c values for fatigue and static loadings, in the case of unnotched beams, the former was found to be 7,5 per cent lower. The difference was attributed to the elastic creep caused by the mean static load. In spite of this difference it could perhaps be concluded that the material had the same criterion of fracture in both fatigue and static loadings, namely the strain-energy release rate.

NOTATIONS

b = width of beam

C = depth of an edge crack or semi-major axis of an internal crack

$( )_c$ = critical . . .

C_o = initial crack length

C_c = critical crack length

d = overall depth of beam

Δ = differences of deformeter readings

e = deformation (dimensions inches)

$\mathbf{e}$ = basis of natural logarithms

[1] Assoc. Professor, Mechanics Department, Technion, Inst. of Technology, Haifa. Formerly at the Dept. of Theoretical and Applied Mechanics of the University of Illinois.

E = Young's modulus

ϵ = strain (dimensionless)

f'_r = modulus of rupture

f'_c = compressive strength

F = force

G = strain energy release rate (dimensions lb/in.)

G_c = critical strain energy release rate (dimensions lb/in.)

η = coefficient of viscosity

h = net depth of beam at notch = d - C

K = stress concentration factor

L = compliance = $\frac{1}{E}$

L_ϵ = strain compliance (dimensions $in.^2/lb$)

L_e = deformation compliance (dimensions $in.^3/lb$)

M_b = bending moment

N = number of cycles

N_{fail} = number of cycles to failure

ν = Poisson's ratio

S = stress level = σ_{max}/f'_r

σ = normal stress

σ_a = stress amplitude = $\frac{1}{2}$ ($\sigma_{max} - \sigma_{min}$)

σ_{max} = maximum fatigue bending stress

σ_{min} = minimum fatigue bending stress

σ_{mean} = mean fatigue bending stress = $\frac{1}{2}$ ($\sigma_{max} + \sigma_{min}$)

σ_n = nominal bending stress at root of notch

σ_{St} = bending stress at onset of instability in static loading

T = surface tension (dimensions lb/in.)

Z = maximum strain-energy per unit volume a material can contain (=resilience)

I. INTRODUCTION

Investigations conducted at the University of Illinois (1,2,3)[2] have shown that the fatigue fracture in mortar beams containing a single aggregate of various types always occur at the cross-section containing the aggregate. Recently Hsu, Slate, Sturman and Winter (4) from Cornell University have shown visually by microscopic examination that in static loading fracture initiates at the aggregate-matrix bond. It thus seems logical to assume that in fatigue too, not only does the fracture occur at the cross-section containing the aggregate, but also that it actually initiates from the aggregate-matrix bond. Moreover, Hsu et al. have shown that some aggregate-matrix separations occur before any loading has been applied to the material. Fatigue fracture therefore initiates from an aggregate because between it and the matrix there is a pre-existent crack or at least will be on the loading of the first cycle. This, however, is still a long way from fracture since for fracture the crack must extend into the matrix. It is therefore necessary to study the propagation of fatigue cracks in the cement mortar and hence this material became the subject of the present investigation.

In order to study the propagation of cracks two methods may be attempted: direct and indirect. The direct method consists of actually viewing the crack and measuring its rate of progress by such techniques as the successive breaking of electric circuits. Staining technique, may be used but the information gained will be only partial. The indirect method consists of measuring strains and subsequently interpreting them in terms of crack lengths. For both the direct and the indirect method it would be necessary to know in advance at which cross-section the crack would develop. For this reason a notch may be introduced in part of the specimens. It is emphasized that this notch will not be to simulate a crack, an undertaking not easy in a material such as mortar. Aside from this object the notch may also serve the following purposes:

(1) Measuring the deformations across the notch will ensure that the changes measured will be only those at the critical area. Better accuracy could therefore be expected.

(2) For reasons later explained the slow extension of a crack will be longer if it initiates from a deep notch (as against a natural shallow notch). This will facilitate more readings and better accuracy.

(3) The notch is considered analogous to the pre-existent crack in concrete mentioned earlier. It is believed that behaviour of concrete beams in fatigue will be very similar to mortar beams with a notch.

(4) The notch can serve as a convenient trough for ink in the staining technique.

When studing the propagation of fatigue cracks, some attention will also be given to the propagation of static cracks and an attempt will be made to find a

[2] Figures in parentheses refer to list of references.

common denominator for the two types of fracture.

Two final remarks: (1) Throughout this work the term "static" is used as the opposite of "fatigue". It is conceded that this is a misnomer, the repeated loading causing a fatigue behaviour is a static and not a dynamic loading. This nomenclature, however, follows the usual practice. (2) The terms "deformation" and "strain" are used here in their U.S. sense i.e. deformation is the change in dimension having a dimension of length while strain is the relative deformation i.e. it is dimensionless.

II. EXPERIMENTAL

1. Apparatus

(1) Fatigue machine. The flexural fatigue machine is shown schematically in Fig. 1. It was capable of applying various degrees of repeated bending loads from slightly over zero to maximum, but was not suitable for reversed loads nor for zero minimum loads, since the beams were supported from above only. The loads were applied by a system of levers providing amplification of load and also some flexibility to the machine. An adjustable connecting rod transmitted the load between the levers which were actuated by a motor-driven variable eccentric. The loading plate with strain-gages mounted on also served as dynamometer. The amplitude of strain was adjusted by the set in the eccentric, while the limits of strain were controlled by the adjustable connecting rod. In the course of fatigue life, readjustments of load were accomplished by varying the length of the adjustable connecting rod. Readjustments of amplitude were not carried out due to the complexity of the operation.

The machine applied approximately 450 repetitions of load per minute and was halted automatically whenever a specimen failed. A counter recorded the number of cycles. The fatigue machine also served for the static loading of beams. In such a case the load was increased by manually adjusting the connecting rod while the eccentric remained stable at bottom position.

The beam was simply supported from above on a 40 in. span and subjected to symmetrical two point loading which provided a test section 10 in. long in which the bending moment was constant.

(2) Static machine. While full length beams were tested statically in the fatigue machine as just described, the half beams resulting from both fatigue and static failure were tested on a separate machine. This machine, shown in Fig. 2, is a manually operated gear and screw machine. The load was transmitted to the specimen through a proving - ring dynamometer and a loading plate.

(3) Deformeters. Two different methods were used for deformation measurements: one was a direct strain measurement by means of a bonded electrical resistance strain gages; and the other was a deformation measurement, which provided average strains, by means of a specially made deformeter shown in Fig. 3. It was made of aluminium and had reduced sections at suitable places. Electrical resistance strain gages mounted on these reduced sections and wired to form a

four arm bridge registered the distortion of the pre-calibrated deformeter. It was held by means of pointed screws mounted in clip angles which were cemented to the specimen. With no load on the specimen a contraction was imposed on the deformeter and the screws were set by lock nuts. Subsequent loadings of the specimen caused reductions in the initial contraction and these were measured by strain indicators as axial deformations. Corrections were subsequently made for the detachment of deformeter from beam.

Deformeters of two different sizes were used: 8 in. long on a 10 in. span for unnotched beams, and 3 in. long on a 4 in. span (which included the notch) for notched beams.

2. Materials

(1) Cement - Type I portland cement.

(2) Sand - The sand was a blend of 83.5 per cent by weight of Wabash River sand and 16.5 per cent of fine lake sand. The fineness modulus of the blend was 2.61.

(3) Mix proportions - The mix was designed for a 28 day compressive strength of 4500 psi, which resulted in weight proportions of 1:3.37:0.67 cement, coarse sand, fine sand; or, an overall ratio of 1:4.04. The water-cement ratio was 0.63. The moisture content of the sand was determined for every batch and a correction was made in each case.

3. Specimens

All beams were 42 x 4 x 2 in., the 4 in. side being vertical both in casting and in testing. For Series C,D and E steel wedges were introduced in the forms to produce triangular notches across the width of the beam. The notches were 0.75 in. deep having a vertex angle of 30 degrees.

From every batch mixed six beams and four 6 x 12 in. control cylinders were cast in steel molds. Beams were virbrated and cylinders were rodded. Special care was taken to have good compaction around the wedges in the production of the notched beams.

All specimens and control specimens were demolded after 24 hours and were then transferred to the fog room where they were moist cured for 67 days. Then they were moved to the constant environment room (74 degrees F and 50 per cent R.H.) for storage until tested in the same room. This storage lasted from 2 to 4 months.

4. Description of Tests

Series A - Thirty one unnotched beams were fatigue tested with a constant minimum tensile stress of 50 psi.[3] The maximum tensile stress varied from 450 psi to 710 psi. The procedure was as follows:

(3) The stresses here and hereafter referred to are the extreme fiber stresses on the beam tension face.

By means of the conecting rod the load was gradually increased from zero to the required maximum with deformeter and strain-gage readings taken versus load. This provided stress-strain characteristic at zero cycles. The eccentricity was then adjusted to give the required minimum stress of 50 psi, and the machine was started to run. It was stopped at 100 cycles and readings of load and strain were taken for both maximum and minimum loads. If a drop of stress from the original value was noticed, then it was reset by adjusting the connecting rod and the strains were again noted. No adjustments of amplitude were made. The stress-strain relationship was again obtained as before, but only within the limits of the minimum to the maximum loads. This procedure was repeated for 500, 2,500, 10,000 cycles and thereafter at reasonable cycle intervals up to failure. Strain-gage readings, when strain-gages were used, were taken together with deformeter readings.

Series B. Sixteen unnotched beams were tested as in Series A (without electrical strain-gages) but with a minimum tensile stress of 150 psi. The maximum tensile stresses varied from 570 psi to 750 psi.

Series C. Sixteen notched beams were fatigue tested with a constant minimum nominal tensile stress of 50 psi. (This nominal stress was calculated from the bending moment applied to the beam using the beam formula. Actually such stresses existed only at great distance from the notch while the measured strain was at the notch. Nevertheless, for designation purposes, the nominal stress will be mentioned.) The maximum nominal stresses varied from 280 psi to 340 psi.

In this test the beams were fitted with the 3 in. deformeter directly over the notch. The procedure was as before except that the beam surface directly below the notch was kept under observation by means of a magnifying glass for developing cracks. (Attempts were made to record the development of cracks automatically by means of electric circuits that break successively as the crack extends through them. Copper wire, 1/1000 in. dia., and thin strips of silver paint used for printed circuits were tried but failed. The propagating crack was so thin that even the extremely thin silver paint did not break when a crack developed behind it).

Series D. Fifteen notched beams were tested as in Series C, but with a minimum nominal stress of 100 psi. The maximum nominal stresses varied from 270 psi to 330 psi.

Series E. Ten notched beams were tested as above, the minimum nominal stress being 20 psi, which was the absolute minimum possible with the machine at hand. The maximum nominal stress varied from 260 psi to 340 psi.

Series F. The static testing consisted of the following:

(1) 7 unnotched beams were tested to failure statically on the fatigue machine. Strains, measured by the 8 in. deformeters, were noted versus loads. Load was applied in increments by the adjustable connecting rod.

(2) 12 notched beams were similarly loaded to failure with deformations measured by the 3 in. deformeters mounted on 4 in. span. Since this span included the notch, the measured deformation was almost entirely that at the root of the notch.

(3) 212 half beams of both notched and unnotched specimens and of both fatigue and static testing were tested for modulus of rupture on the static machine. No strains were measured.

(4) Companion cylinders, 27 of the unnotched and 31 of the notched beams, were crushed on a hydraulic static machine (type Riehle) to determine the compressive strength at the age at which the beams were fatigue tested.

(5) In order to be able to interpret the fatigue strain readings in term of crack lengths, the effect of crack length on the beam compliance was investigated as follows:

A relatively blunt notch of a certain depth was made at the center of the constant moment region by an ordinary concrete saw without wetting. The beam was then mounted on the fatigue machine with green india ink in the trough of the notch which was plugged at both ends by wax. (It was previously ascertained that the ink did not soak into the pores of the material). The beam was then loaded by the adjustable connecting rod at equal increments. Deformation increments, as measured by the deformeter spanning the notch, were noted. Loading was continued as long as the deformation increments remained constant and some measure beyond this point; carefully, however, to avoid fracture. The beam was then left for about 20 minutes under load giving a chance for the ink to penetrate into the crack which had formed at the root of the notch. The load was then removed and the remaining ink in the trough sucked out. The beam was then again loaded and deformations versus loads noted up to failure. After failure the depth of ink penetration was measured and the compliance as derived from the second loading sequence was attributed to this crack length. The same procedure was repeated several times for saw notches of different depths which caused natural cracks of different depths.

III. RESULTS AND ANALYSIS

5. Series A

Strain results of one representative beam out of the thirty used in this series are shown in Fig. 4. ϵ_{max} and ϵ_{min} are respectively the maximum and minimum strains on the beam tension face as measured by the deformeter. The electrical resistance strain gages gave almost identical results and these are therefore omitted. L_ϵ is the compliance as obtained by dividing $\epsilon_{max} - \epsilon_{min}$ by $\sigma_{max} - \sigma_{min}$.

It should be noted that $\sigma_{max} - \sigma_{min}$ did not remain constant throughout the fatigue life as it would have done had the machine been a true stress machine, but slowly decreased with the increasing cycles. Table 1 illustrates the way L_ϵ was derived. C is the crack depth from the beam tension face, as was derived from the compliance L_ϵ and the results of Series F(5), namely the effect of crack-length on compliance, which will be presented later.

Fig. 5 shows the stress-strain characteristic of one typical beam of this series as changed throughout its fatigue life. It should be noted that the initially curved line becomes straight after the first cycle and that the modulus gradually diminishes with N, in agreement with the compliance results presented in Fig. 4.

The S-N curve of this series is shown in Fig. 6. For a reason to be explained later, S was taken as the ratio of σ_{max} to the mean static strengths of all the unnotched beams (excluding Series B).

No visual evidence of impending fatigue failure was achieved, due perhaps to the fact that in an unnotched beam there was no clue as to where to focus the inspection.

6. Series B

The sixteen beams in this series were cast at a much later date than the rest of the specimens in this investigation. Although the mix proportions were exactly the same, the materials were from a different consignment. The mean static strength of this series is much higher than those of the other series (see Table 2) and the indication was that the elastic modulus was also higher. Since no static testing (other than the mentioned "halves") of this obviously different material was done and no compliance-crack length dependence was determined, it was not possible to evaluate crack-length for this series. In any case such crack-lengths in this case would not have been very useful since no equivalent static values were available for comparison. For this reason the only result presented for this series is the S-N relationship in Fig. 7.

7. Series C.

The results of this series, as well as those of all notched beams, are presented in terms of deformation rather than strain. This is because in this case the strain is confined to a very small area at the root of the notch and its true magnitude can not be easily determined. The maximum and minimum deformations e_{max} and e_{min}, the compliance L_e (deformation-compliance, as distinct from strain-compliance in the case of unnotched beams) and the effective crack-lengths C, of one representative beam is shown plotted against N in Fig. 8. In this graph e_{max} and e_{min} are measured quantities while L_e and C were derived in a manner explained previously for unnotched beams.

Fig. 9 shows the stress-strain characteristic of the same beam as affected by cycles. It should be noted that at N = 0 it is quite concave downwards

whereas the following curves are all straight lines. Also, that the slopes of these lines diminish appreciably with cycles.

The S-N curve for Series C is shown in Fig. 10. The ratios S were based on the mean static strength of all the notched beams in the study. Beams for which C_o, the initial crack as derived from the compliance of the first loading cycles (the procedure will be described later), was greater than 1 inch were marked by a black point. This value was chosen arbitrarily but it served as a rough guide as to which points to exclude from the curve. The reason for this, as well as method for correction,will be discussed in the next chapter.

In this series, as in all the others dealing with notched beams, a frequent inspection by means of a magnifying glass revealed the existence of a crack long before final failure. The crack, emerging from the root of the notch could be seen pulsating with the repeated loadings and unloadings. Careful inspection could also roughly determine the extent of the crack and its gradual progression with time. However, no results to this effect are presented here.

8. Series D

Fig. 11 shows the deformations, compliance, and crack-length of one representative beam out of the fifteen used in this series. Fig. 12 is the stress-strain versus cycles of the same beam. Fig. 13 presents the S-N relationship of this series. Here again specimens which had an initial crack deeper than 1 in. were not included in the curve.

9. Series E

Fig. 14 shows the deformations, compliance and crack length of a sample beam of this series. Fig. 15 is the stress-strain of the same beam during fatigue life. Fig. 16 presents the S-N relationship. Here again points for beams in which $C_o > 1$ in. were excluded from the curve.

10. Series F

The static stress-strain curves up to fracture of three representative unnotched beams are shown in Fig. 17. The static stress-strain curves of four representative notched beams are shown in Fig. 18. The last strain reading in the case of a notched beam was not accurate due to the rapid change of strain towards failure. In most cases the true value was higher than the recorded one.

The results of static strength determinations are summarized in Table 2 where only mean values are presented. The "half beams" include the remaining halves of both static and fatigue breakings. The ages at which they were tested correspond approximately to the age of fatigue testing. It should be realised that f'_r as determined from full notched beams is only an apparent value due to the disregarded notches. Standard compressive strengths of the companion cylinders are also presented.

The various S-N curves shown previously were all based on the overall means of Table 2. It was at first considered best to relate each fatigue strength

to the static strength of the same beam. Then it was thought that the mean static strength of the batch would serve as a basis. However, after finding out that neither of these methods improved the scatter of the S-N curves, it was decided to use the total mean as a basis. It is now believed that since strictly speaking the static strength serving as a basis should be that at the same cross-section where fatigue fracture eventually took place, taking the same batch or even the same beam as a basis should not be an improvement. This is because the variations of strength between several cross-sections on the same beam is not smaller than variations between different beams as could easily be verified from the results. In the case of the notched beams, since only nine f_r' values were available for full beams, the following method was used: the mean of the nine was determined (column (1)) and also the mean of the "halves" belonging to the same nine beams (column (4)). The ratio of these two means was 1:2.38. Then, the mean strength of all the "halves" resulting from notched beams (numbering 106) was determined and divided by 2.38. The result was therefore the mean f_r' for a full notched beam based on all the notched beams in the investigation. The f_c' values were not made use of at all.

The results of the investigation of compliance versus crack-length are shown in Fig. 19 and 20. The first of these graphs presents the stress-strain curves of beams with natural cracks of varying depths which were obtained in preceding loading sequences as described previously. The inverse slope at the origin of each of these curves was plotted against the corresponding crack-length in Fig. 20. The first point in this plot, viz for C = 0, was obtained from the mean of the unnotched beams. The point for C = 0.75 in. was obtained from the mean of the notched beams with the standard notch of this investigation, i.e. having an angle of 30 degrees and a depth of 0.75 in. Fig. 20 thus presents the dependence of the compliance on the crack-length. The compliance has two scales: one is a strain-compliance with dimensions in^2 /lb for the unnotched beams, and the other a deformation-compliance with dimensions in^3 /lb for the notched beams. Fig. 20 has been used in all the previously presented fatigue results for evaluating C from L_e or L_ϵ .

The need for the L-C curve arose from the failure to measure directly the crack propagation during the fatigue process. As already mentioned the method of successive breakings of electric circuits, both of thin copper wire and of silver paint, due to crack growth has failed. The use of ink during the fatigue life to indicate the critical crack-length would have been very convenient except that it was considered that the ink would interfere with the material surface tension. In the method used here the ink was not in contact with the newly formed surfaces until it was given time to penetrate which was some time after these surfaces were formed.

For reasons to be explained in the next chapter, it was considered instructive to evaluate for all fatigue beams, both unnnotched and notched, the quantities $\sigma_{max}.C_c$ and $\sigma^2_{max}.C_c$. The value C_c (in inches) would be that where the C curve intersects with the failure line in each of the fatigue graphs. σ_{max} would simply be the maximum stress (in psi) applied to the particular beam. Table 3 shows this operation for almost all the fatigue beams in this investigation.(4) It is significant that an almost uniform $\sigma_{max}.C_c$ value was obtained especially in the case of the notched beams, and also a fairly

(4) The reason why some beams were excluded from this operation will be explained in the Discussion

uniform $\sigma^2_{max}.C_c$ value.

For the same reason, to be later discussed, it was also considered instructive to compare the fatigue $\sigma_{max}.C_c$ and $\sigma^2_{max}.C_c$ with the static $\sigma_{st}.C_c$ and $\sigma^2_{st}.C_c$. In the case of unnotched beams tested statically (Fig. 17), σ_{st} was the fracture stress and C_c was derived in the following manner: the compliance L_ϵ at the point of fracture was obtained from the graph. This was then used in the L-C curve in Fig. 20 for obtaining the equivalent C. In the case of notched beams tested statically (Fig. 18), σ_{st} was taken as the stress at which rapid strains commenced (the points of singularity in the curves) and C_c was obtained through the compliance at the same point, again using Fig. 20. These operations and the results are presented in Table 4.

The results of Table 3 and 4 should be viewed together. They are discussed in the next chapter.

IV. DISCUSSION

11. The Griffith-Irwin Theory Applied to Concrete

Although the main business of this investigation is with fatigue, it might be instructive to also dwell a little on the static fracture mechanism of concrete. The author has dealt with this matter elsewhere (14) and will mention here only the essentials:

The Griffith equation for an elliptical flaw normal to a tensile field in a plane stress case

$$\sigma = \sqrt{\frac{2ET}{\pi C}} \qquad (1)$$

is represented graphically in Fig. 22. For a crack whose semiaxis is C_1 to grow spontaneously, a stress σ is required such that

$$\frac{d}{dC}\left(\frac{\pi C^2 \sigma^2}{E}\right) = \frac{d}{dC}(4CT) \quad . \; . \; . \qquad (2)$$

A crack shorter than C_1 will require a greater stress. In an ideal elastic material this is all that has to be known and the quantities E and T solely determine the material toughness. In real materials, however, most of the elastic energy is not transformed to surface energy but is dissipated in some other way. In metals almost one hundred per cent of the energy is dissipated by plastic deformations in the highly stressed zones near the tips of the crack. Accordingly the crack will not grow unless the rate of elastic energy release will equal the rate of energy absorption by plastic strains. But even then the growth will still not be spontaneous for the plastic zone grows together with the crack so that the requirement of energy per unit length of crack will increase. It is therefore necessary to gradually increase the stress in order to force the crack to expand. This is illustrated schematically in Fig. 23 where the energy-requirement-curve has an increasing slope, distinct from the

constant slope of Fig. 22. For the initial crack length C_o, when the stress is σ_o, the energy release and energy requirement curves are parallel (on the vertical line through C_o) so that eq. (2) is satisfied. But to the right of this point the two curves diverge so that no further growth is possible until the stress is raised to σ_1. Here again a limited growth is possible (since the two curves are parallel on the vertical line through C_1) but after that the stress has to be further raised. Thus the crack is forced to grow by raising the stress continuously. The figure shows this as a stepped process. Actually the growth of both stress and crack length is continuous. Beyond C_4 no further raising of stress is required for the crack to grow because to the right of this point the slope of the energy release curve is already larger than that of the energy requirement curve (the two curves converge). The crack will therefore run spontaneously beyond C_4 which will thus become the critical crack length and σ_4 will be the breaking stress. If the strain-energy release rate (the slope of the curve) at this point of instability commencement is measured, it will be found to be a material property. The strain-energy release rate is usually designated by G and its critical value by G_c. G_c is thus the resistance of metals to brittle fracture. When the third dimension is considered G has the dimension of a force and is sometimes referred to as the "driving force". In actual fact it is the energy released for the formation of a unit new surface; and since it is measured at the onset of instability it includes the total requirement of energy. G_c replaces E in Griffith's equation and it can be seen from Fig. 23 that in tension

$$G_c = \frac{2\pi C_c \sigma_{tens.}^2}{E} \qquad (3)$$

In concrete, an analogy can be found to the case of metals. It is not claimed that plastic strains accompany the crack growth as in metals, for concrete is a typical non-plastic material, but that in concrete too, a large energy dissipation is involved. In the highly stressed zones, discrete cracks are formed which do not necessarily combine with the main crack. This means that in order to expand the main crack the strain energy should provide for more surfaces than those required by the main crack alone. Kaplan (5) has shown that the total energy release in concrete is approximately twelve times the newly formed surface energy in the main crack. Pernaps it could therefore be surmised that the total new surface area is twelve times the surface area of the main crack alone. Phenomenologically, nevertheless, the behaviour is similar to that of metals and in concrete too there exists first the slow growth and then the fast growth stages. But in concrete another factor enters: heterogeneity. Aside from being controlled due to increase in energy demand for microcracking, the growth is also often checked by encountering an obstruction such as an aggregate. In most aggregates the surface tension is higher than in the cement paste so that when the crack penetrates an aggregate the demand of energy is suddenly increased. If the crack deviates around the aggregate then the demand is also appreciably increased for the actual surface formed is much greater than the effective surface. A case of a crack developing in a bi-phase material is illustrated in Fig. 24. The crack C_o will start growing under a stress σ_o but when reaching C_1 the energy demand will suddenly increase. It will therefore be necessary to increase the stress to σ_1 for the crack to continue growing.

In spite of this complication, it may be quite possible to measure the critical strain-energy-release-rate, G_c, for concrete, and it may be found that for concrete, as in metals, it is a material property. Kaplan (5) has already made the first step in this direction. Two ways are available for G_c determination: (a) To measure the critical crack-length C_c, i.e. the maximum extent of slow growth, and the breaking stress $\sigma_{tens.}$ and to calculate G_c from eqn (3); and (b) To measure the change of compliance L as a function of crack length and the breaking force F and to calculate G_c from Irwin's (6) eqn.

$$G_c = \frac{1}{2} F^2 \frac{dL}{dC} \quad . \; . \; . \qquad (4)$$

The most suitable test for this would be the tensioning of sharp notched specimens, but flexure may be also used.

The fast growth of a crack is defined as that which is being fed by the energy contained in the strained body without contribution from an outside source. For this reason the capacity of elastic straining of the body is important in determing the critical point at which slow crack growth becomes fast. Glucklich (7) has shown that the introduction of a spring between a compression specimen and the machine causes cracks to become fast-growing right from the start. The reasons for this are: (a) When motion due to cracking starts, the potential energy of the spring becomes kinetic energy capable of doing work against any obstruction that may be encountered or satisfying any rise in energy demand. Glucklich referred to this as a "first crack mechanism" as distinct from the "cracking mechanism" which occurs as a result of gradual and slow cracking process.

12. The Static Bending Fracture

The stress-strain curve to fracture of mortar beam is almost a straight line. Some investigators (8,9) claim that it is perfectly straight even for concrete, but careful measurement in this investigation has shown deviation from linearity at approximately 50 per cent of the breaking stress. In the case of notched beams the nonlinearity was much more pronounced and Fig. 19 shows that it increases with the depth of the notch.

The fracture of an unnotched beam initiates from a natural small sized notch and since from eq (1) σ^2 is proportional to 1/C this notch starts growing at relatively high stress. This will be a slow growth with the stress increasing until the quantity

$$G = \frac{\pi C \sigma^2}{E}$$

will reach its critical value when fast propagation, or fracture, will take place. The deviation from linearity will be due to the slow growth which, however, will be small in an unnotched beam. In the case of a very smooth surface, the stress-strain curve will look even more linear. In the case of a notched beam the start of growth will be at a much lower nominal stress and

this fact is responsible for the difference in the two stress-strain characteristics. While in an unnotched beam when the slow growth is in progress the entire beam is highly stressed, in a notched beam the high stress is concentrated around the notch and the rest of the beam has a much lower stress level. This is analogous to the two loading methods mentioned in the preceding section, with and without a spring. In an unnotched beam the energy content in the beam is sufficient to maintain a constant stress when fast propagation takes place so that fracture can happen spontaneously. In a notched beam, on the other hand, the energy reserve is very limited and when fast propagation commences the stress level rapidly drops. In order to accomplish fracture, therefore, the stress must be maintained by following up with the loading machine. The difference in the two behaviours can be seen by comparing Fig. 17 with Fig. 18. Up to a certain point they are qualitatively the same, but at that point the unnotched beams fail abruptly while in the notched beams the curve continues though at a shallower slope. The fact that in a notched beam the stress can be raised beyond this point is due to the fast straining when viscous resistance is probably mobilized.

In consequence, the point of instability is at the termination of the curve for the unnotched beams and at the sharp change of slope for the notched beams. (It is realized that continuity of this curve must be maintained. The curves were drawn with sudden changes of slope to enable the pinpointing of the critical stresses). The stress at this point was designated σ_{St} and the crack length C_c. C_c was obtained indirectly from the compliance L (the inverse of the secant modulus) at the point and the L-C curve in Fig. 20. The values $\sigma^2_{St}.C_c$ for each beam appears in Table 4. The reason for this operation may now be appreciated as obviously this value is a measure of G_c. Indeed, as the table shows, all beams have approximately the same value. Moreover, it appears that there is no great difference between the results of notched and unnotched beams, which confirm the suggestion that it might be a material quantity. For comparison, $\sigma_{St}.C$ values were also determined and while the dispersion within each group was better than for $\sigma^2_{St}.C_c$, the difference between the groups was too great for $\sigma_{St}.C$ to be significant.

With the realization that $\sigma^2_{St}.C_c$ is a significant quantity, G_c may be determined for the material used in this investigation. For the unnotched beams the equation to be used is:

$$G_c = \frac{\pi C_c \sigma^2 (1-\nu^2)}{E} \qquad (5)$$

This eq differs from eq (3) in that it applies to an edge crack instead of an internal crack and in that it provides for plane strain conditions. σ can be taken as the bending stress at the extreme fibers of the beam since the pertinent notch is fairly shallow.

For the notched beams, since the notch is approximately 20 per cent of the overall depth, the effects of the reduced cross-section and the non-uniformity of stresses must be taken into account. The eq used by Winne and

Wundt (10)

$$G_c = \frac{\sigma^2_n h (1-\nu^2)}{E} f(\tfrac{c}{d}) \qquad (6)$$

may be used. Here σ_n is the nominal stress at the root of the notch(assuming linear distribution in the reduced cross-section), d is the overall depth and h is the net depth (= d - c). For the function $f(\frac{c}{d})$ they provide a graph in terms of $\frac{c}{d}$.

G_c from unnotched beams

From the slopes at the origin in Fig. 17 and from other beams tested statically but not shown,it was found that E = 3.33 x 10^6 psi. Compression tests with the same material (not described here) have shown Poisson's ratio, ν = 0.20. Table 4 shows a mean $\sigma^2_{St}.C_c$ value of 121,000 lb^2/in^3. Substituting these values in eq (5) yields

$$G_c = 0.1100 \text{ lb/in.}$$

G_c from notched beams

In attempting to use eq (6) it must be realised that C can not be taken as 0.75 in. since the slow crack extension must also be considered. C will therefore be taken as the mean in Table 4, i.e. C = 0.946 in. Hence h = 3.054in. and $\frac{c}{d}$ = 0.2365. Winne and Wundt's curve gives $f(\frac{c}{d}) = 0.380$. To calculate σ_n if b is the width of the beam

$$\sigma = \frac{6M_b}{bd^2}$$

and

$$\sigma_n = \frac{6M_b}{bh^2}$$

hence

$$\sigma_n = \sigma \frac{d^2}{h^2} = 1.715\,\sigma$$

σ is taken as the mean from Table 4, i.e. σ = 343 psi. Therefore, σ_n= 587.5 psi. Taking ν = 0.20 as before and E = 3.33 x 10^6 psi and substituting all these values in eq (6) yields

$$G_c = 0.1150 \text{ lb/in}$$

The two results are almost identical. It must therefore be concluded that G_c is the material constant and not $\sigma^2_{St}.C_c$. The difference in the $\sigma^2_{St}.C_c$ values between notched and unnotched beams (Table 4), which was almost ignored before, now becomes significant. These values are greater for unnotched beams for in a case of shallow notches the stress field can be considered uniform, while in medium notches the stress gradient must be considered. Winne and Wundt's curve for $f(\frac{c}{d})$ (which is ascending with respect to $\frac{c}{d}$) takes care of notches of all depths. Thus, the G_c value for the unnotched

beams could also be calculated using eq (6), rather than eq (5), but then $f(\frac{c}{d})$ would be less than 0.380. Since, however, $\sigma^2_{St}.C_c$ for unnotched is larger than for notched beams, G_c would still be the same, as indeed happened here.

13. The Fatigue Bending Fracture

The ϵ_{max} and ϵ_{min} curves in the fatigue of unnotched beams (as examplified by one beam in Fig. 4) are almost parallel. This may give one the wrong impression that the compliance of the beam does not change during the fatigue life. This excludes all possibility of cracking. Such impression must lead one to the conclusion that the only thing that happens to the beam during fatigue is creep. Indeed, comparing e_{min} with creep caused by a static load of $\frac{1}{2}(\sigma_{max} + \sigma_{min})$ revealed that about 80 per cent of e_{min} is creep. But why should creep in fatigue reduce the strength to about 60 or even 50 per cent? The fallacy is revealed when attention is focused on $\sigma_{max} - \sigma_{min}$ during the fatigue life. The machine used in this investigation was not a stress machine and although σ_{max} was constantly adjusted the difference $\sigma_{max} - \sigma_{min}$ gradually decreased. However, it was not a totally strain machine either and the difference $\epsilon_{max} - \epsilon_{min}$ slightly increased during fatigue. For this reason it was necessary to determine the ratios $(\epsilon_{max} - \epsilon_{min})/(\sigma_{max} - \sigma_{min})$ which are, of course, the compliances. This is illustrated in Table 1. Plotting the compliances has shown that in all cases they increase during fatigue life. No reason other than cracking could explain this phenomenon. The stress-strain characteristics at various stages of fatigue life as examplified by Fig. 5 for unnotched beams and by Figs. 9, 12 and 15 for notched beams, have confirmed this hypothesis. As shown before , the static stress-strain curve of a beam will be concave with respect to the strain axis, more so in the case of a notched beam. In Figs. 5, 9, 12 and 15, the stress-strain at N = 0 is concave, more so in the last three which represent notched beams. During the first fatigue cycle, therefore, some cracking, corresponding to the stress level employed, takes place. The following curves are perfectly linear, which indicates that the cracking for that stress level has ended. However, inspection of the slopes of these straight lines shows that they decrease with cycles. This observation agrees with the increasing compliance reported before and can be explained only by the assumption that the cracking, which has stopped when the stress reached its maximum value in the first cycle, is continued due to the repeated cycles. In other words, a certain amount of cracking can be brought about by either a relatively high stress applied once, or a lower stress repeated many times. In the second case the repetitions of loading will accomplish what the lower load missed. This hypothesis will explain why fatigue limit (if exists for concrete) is at approximately 50 or 60 per cent; below this load no cracking takes place in static loading and the repeated cycles will have no cracks to propagate. A mechanism by which such propagation is possible will be discussed elsewhere.

When it was realized that the repeated loading propagates cracks, it was attempted to observe and measure this propagation. Notched beams were thus introduced so that it will be known in advance where fracture might develop. However, the various propagation measuring techniques have failed and the only

observation made of the cracking progress was visual: A very fine crack could be seen gradually increasing in length with cycles. It was then decided to use the strain measurements, which in the case of notched beams were concentrated almost entirely at the notch, for determining the crack length. To exclude creep, the strain differences, or compliances, were used and the dependence of compliance on crack-length was statically determined. As it was almost impossible to make a notch that will simulate crack in concrete, the technique of producing natural cracks already described was employed. When the crack-length development with cycles was thus obtained, two crack lengths were considered important: (1) C_o, the crack-length before loading, and (2) C_c, the crack-length at failure. The latter will be considered first.

When C_c was tabulated opposite the fatigue stress σ_{max} (Table 3), it was observed that for a beam with high σ_{max} there was a low C_c and vice versa. The values $\sigma_{max}.C_c$ were therefore determined and tabulated. The result was quite uniform, especially for the notched beams. However, the values obtained for notched and unnotched beams were entirely different. This created doubt as to the significance of $\sigma_{max}.C_c$. The value $\sigma^2_{max}.C_c$ was then similarly tried and although the scatter of results was somewhat greater than for $\sigma_{max}.C_c$, there was only a small difference between notched and unnotched beams. However, as in the case of static fracture, it should not be anticipated that $\sigma^2_{max}.C_c$ would have quite the same value in notched and unnotched beams, for while in the latter it is almost a case of uniform stress, in the former the reduced cross-section should be considered. In proceeding to compare fatigue with static results, one should therefore compare separately the unnotched and the notched groups. The tables show for unnotched beams $\sigma^2_{max}.C_c = 110{,}800$ lb^2/in^3 and $\sigma^2_{St}.C_c = 121{,}000$ lb^2/in^3; for notched beams $\sigma^2_{max}.C_c = 105{,}700$ lb^2/in^3 (mean of three notched series) and $\sigma^2_{St}.C_c = 111{,}500$ lb^2/in^3. These values compare quite well (a possible explanation for the difference that nevertheless does exist between static and fatigue results will be presented towards the end of this chapter) and it may therefore be inferred that in fatigue the strength determining property is also G_c. This value could be evaluated separately for each beam from the fatigue results using again eqs (5) and (6). However, this will not be done here due to the uncertainty with regard to $f(\frac{c}{d})$. For the unnotched group, however, it can be done and the mean $\sigma^2_{max}.C_c$ will be used for that purpose:

Substituting $\sigma^2.C_c = 110{,}800$ lb^2/in^3, $\nu = 0.2$ and $E = 3.33 \times 10^6$ psi in eq (5) yields

$$G_c = 0.1020 \text{ lb/in}$$

This value is approximately 7.5 per cent less than the G_c obtained in static testing. A possible explanation will be presented later.(5)

(5) Although not done here, the computation of fatigue G_c on the basis of the three notched groups will yield values averaging 10% higher than their static counterparts. The author does not know how to account for this except perhaps by assuming that the C_c values in these groups, having been obtained through compliances, are the effective crack lengths and thus slightly larger than the true ones.

It thus becomes clear that the function of the repeated loading in bringing about fracture is to increase the crack length to a value which together with the lower fatigue stress will combine to a value close to the static G_c. Therefore, results of static tests may be used in predicting fatigue behaviour. Thus for certain fatigue load, the critical crack-length C_c can be predetermined and if the compliance-crack length relationship is available, the compliance at failure can be predicted. This may be helpful in estimating at every stage of fatigue life the closeness of failure.

Inspection of Table 3 reveals that the coefficient of variation for both $\sigma_{max} \cdot C_c$ & $\sigma^2_{max} \cdot C_c$ is greatest in the unnotched beams. There may be three reasons for this, only the last two of which are significant: (a) In the unnotched series there had been quite a long lapse of time between the testing of the early (with the low serial numbers) and the late specimens. The trend of the $\sigma^2_{max} \cdot C_c$ values is to increase slightly with the age of the specimens. (b) The compliance determination in the case of unnotched beams was on the entire constant moment region. In the case of notched beams the compliance was determined across the notch where the crack developed. Obviously in the latter case the crack-length effect on the compliance was more pronounced and hence better accuracy could be expected. (c) Since crack-lengths were determined from the compliance by means of the curve in Fig. 20, the accuracy of this curve was important. While in the case of notched beams the portion of the curve used was between C = 0.75 and C = 1.30, where the curve is rapidly ascending, in the case of unnotched beams the curve was used between C = 0 and C = 0.30. In this region the curve is almost horizontal so that compliance is very insensitive to crack-length and mistakes in determining the latter are quite probable. It is to be anticipated that concrete, which has pre-existent cracks between aggregates and matrix, will in this respect behave as the notched beams in this investigation so that the compliance vs crack-length technique will be quite dependable.

In this connection it should perhaps be remarked that all references to crack-length in fatigue are intended to mean effective-crack-length. As already mentioned, a process of micro-cracking accompanies the growth of the main crack and this also contributes somewhat to the increase of compliance. However, this fact does not reduce the practical usefulness of the technique, since in the static determination of $\sigma^2_{St} \cdot C_c$, C_c also includes the effect of micro-cracking.

The other important crack-length, C_o, will now be discussed. The graphs show that C_o for the unnotched beams varied from 0.12 to 0.24 in. These therefore are the effective depths of the natural notches that exist on the unfinished mortar surface. In some of the beams (not those presented) C was indeterminable for the following reasons: It will be remembered that the C = 0 point

on the L-C curve was determined from the mean compliance of the unnotched beams. In those beams in which Young's modulus was higher than the mean, the compliance fell below $L = 0.30 \times 10^{-6}$ in^2/lb and C_o could not be determined. In some beams no C value could be determined at all and they were excluded from the analysis in Table 3.

The C_o values in the notched beams varied from 0.75 to 1.10 in. In most cases it was more than 0.75 in., the design depth of the notch. It is believed that in most beams cracks developed at the root of the notch before loading was started. In some cases it may have been caused by careless handling, but in most cases it is attributed to concentration of shrinkage at the root of the notch where more free surface per unit volume is available. These initial cracks were made visible in many cases by the deposition of white calcium carbonate on the surface below the notch.

Since the importance of crack-length on the fatigue strength of beams is now realized, it will be appreciated that specimens with deep pre-existent cracks have low life expectancy. For this reason all beams with initial crack lengths greater than one inch, were excluded from the S-N curves. This has much improved the scatter of the points and was quite legitimate as one could not expect a beam with an exceptionally large crack to have equal weight with other more normal beams. In actual fact all S-N curves may be improved if all the specimens are placed in the same initial position. This can be done in the present case by adding to each beam's N_{fail} the number of cycles required to extend a crack from 0.75 in to its C_o value.

In discussing the S-N curves two other reasons for the high scatter should be mentioned: One is the uncertainty with regard to the static strength. The fatigue strength should be related to the static strength at the same cross-section (actually, at the same crack), and this, of course, is impossible. The second reason has to do with a deficiency of the testing machine: since readjustments of load were not automatic, N_{fail} was to a large extent dependent upon how often readjustments were made. In several cases failure followed soon after such readjustment ; the beam would have probably lasted much longer had this act been further delayed.

14. The effect of the mean static stress

The stress $\sigma_{mean} = \frac{1}{2} (\sigma_{min} + \sigma_{max})$ is acting statically while a stress amplitude of $\sigma_a = \frac{1}{2} (\sigma_{max} - \sigma_{min})$ is cyclic. Glucklich (11) has shown that in a Kelvin body (cement mortar can be represented rheologically to a first approximation as a Kelvin body) with a rheological equation

$$\sigma = E\epsilon + \eta\dot{\epsilon} \qquad (7)$$

η being the viscosity coefficient, the static breaking load is time dependent as follows:

$$\sigma = \frac{\sqrt{2EZ}}{1 - e^{-E \cdot t/\eta}} \qquad (8)$$

In this equation Z is the maximum strain energy which a unit volume of the material can absorb and is a material constant, and e is the base of natural logarithms. Thus in a Kelvin body a delayed fracture can take place under a static load smaller than the normal breaking load. σ_{mean} therefore contributes towards fatigue failure but the effect is time rather than cycle dependent. Also, since most of the delayed elasticity which causes the delayed fracture occures with concrete a short time after loading, this contribution is felt only at the initial stages of the fatigue life. This also explains the limited effective durations of rest periods reported by Hilsdorf and Kesler (12). But the effect of σ_{mean} is even greater. Consider a sinusoidal complete stress reversal loading (Fig. 25 (a)) and assume the existence of a crack at a distance from the neutral-axis where the fiber stress is σ. When the side of the beam which contains the crack is in compression the crack closes and the stress at its tip is $-\sigma$. On reversal of load the crack is in a tensile field and it opens. The stress then at the tip is $K\sigma$, where K is the stress-concentration factor. The stress-time relationship at the highly stressed zone is therefore as shown in Fig. 25 (b). It now appears that at that important place (inasmuch as it is where the damage is done) σ_{mean} is not zero even in the case of complete stress reversal, in fact it can be shown to be

$$\sigma_{mean} = \frac{\sigma}{\pi}(K-1) \qquad (9)$$

In tests such as those made in this investigation, where the cracked side of the beam is always in tension, the effect is, of course, absent, but in all cases where there are some load reversals, not necessarily complete, it must be realized that the mean stress is much higher than that apparent from macroscopic considerations. Therefore, in <u>all</u> cases of repeated loading, whether complete, partial or non-reversal, there is a high static load which contributes towards the fatigue failure. The argument often used to contradict the creep theory, that the fatigue effect is equal for reversed and one-side loading, is therefore not valid.

The effect of the mean static load just described may help to understand why $\sigma^2_{max}.C_c$ was a little smaller than $\sigma^2_{St}.C_c$ (or why fatigue G_c was smaller than static G_c) in the case of unnotched beams. In static loading stress is the only agent of destruction; in fatigue the effect of time, or creep is added and thus the apparent toughness of the material is reduced.

Some observations made by various investigators in the fatigue study of concrete may now be understood. The effect of rest periods has already been mentioned. Murdock and Kesler (13) have reported that by increasing the range of stress the fatigue strength is decreased. This is confirmed in the present study by Fig. 21 where the S-N curves of three series are superimposed on one another. However, while towards failure the fatigue strength is indeed reduced, at early stages the effect is opposite. This may be explained by the effect of the mean static stress which is obviously reduced when the lower limit of the fluctuating stress is reduced. Thus at early stages, when the effect of the mean static stress is predominant, increasing the range increases the strength. At later stages the cyclic stress is predominant.

Most investigators report a fatigue limit in concrete between 50 and 60 per cent, although some (13) have not detected such limit at 10 million cycles. In the present study also no such limit was observed although stresses were not reduced below 60 per cent. However, a fatigue limit of 50 to 60 per cent agrees with the minimum load at which cracking starts in static loading as was observed in this as well as in many other works.

V. SUMMARY AND CONCLUSIONS

Six series of tests, five in fatigue and one static, were conducted with cement mortar beams with the object of gaining some understanding of the principles underlying fatigue failure. The repeated sinusoidal loading was such that the tested region was in pure bending. In two series unnotched beams were loaded with different σ_{min}. In three series notched beams were loaded with different σ_{min}. In all cases deformations were measured throughout fatigue life on the tension face of the beam for both σ_{max} and σ_{min}. Stress-strain characteristics were also determined at various stages of fatigue life. S-N curves were obtained for all series. In the static series, control beams were bent to failure to obtain f'_r, the "halves" of the fatigue were similarly utilized and companion cylinders were crushed for f'_c. In addition the static stress-strain characteristic of beams, both notched and unnotched, were carefully obtained. The notch was of the same dimensions in all cases: triangular, 3/4 in. deep and including an angle of 30°. It was located in the center of the constant moment region, on the tension face. The object of the notch was not to simulate a crack but to predetermine the failing cross-section. In the static series a test was also conducted to obtain the correlation between crack-depth and compliance. For this, natural cracks of varying depths were produced.

The deformation measured during fatigue in all series were transformed to compliance and then translated to crack-lengths. The crack-lengths were in particular examined at two points; at start of test and at failure. The first was important for the improvement of the S-N curve, and the second was paramount in determining the material fatigue toughness.

The critical strain-energy-release-rate (G_c) was determined statically and compared with its fatigue counterpart.

The following conclusions could be drawn from the results of the investigations:

(1) The flexural static stress-strain curve of beams without artificial notch (but with natural small notches) is <u>not</u> a straight line. The non-linearity is due to slow crack extension. The fast crack extension is almost acoustic in speed and hence the curve terminates abruptly.

(2) The flexural static-stress-strain curve of beams with artificial medium sized notches is qualitatively the same but the curvature is more pro-

nounced. In addition, there is an almost sudden reduction of slope of the curve before final fracture. This is caused by the fast crack extension which in this case is nonspontaneous due to relief of stress.

(3) The critical strain-energy release-rate (G_c), when measured from the highest point of the curve in unnotched beams and from the point of change of slope in notched beams is almost identical, confirming the ideas expressed in (1) and (2).

(4) In fatigue the first cycle stress-strain-curve is as described. The following ones are straight with the modulus gradually decreasing towards failure. This is presumably the result of the crack growing with cycles.

(5) The growth of the crack with cycles was visually observed.

(6) Beams with deep pre-existent crack have a short life expectancy in fatigue. The S-N curves may be greatly improved if all the specimens are placed in equal initial position from the notch length aspects.

(7) The effect of range of stress is such that for long fatigue life the decrease of σ_{min} reduces fatigue strength, but for short life it increases the strength. The second half of the statement is explained by the action of the mean static stress through the mechanism of delayed-elasticity.

(8) In each of the fatigue series the product of the maximum stress and the critical crack length ($\sigma_{max}.c_c$) is almost a constant number, but is not the same for notched and unnotched beams.

(9) In each of the fatigue series the product ($\sigma^2_{max}.c_c$) is also almost constant, although the variation is a little greater. However, the difference between the notched and the unnotched groups is in this case small.

(10) The static strength determining property of the material is however G_c, the strain-energy release rate, and not $\sigma^2.c_c$. The G_c values in this investigation were almost identical whether obtained from notched or unnotched beams.

(11) Judging from the behaviour of unnotched beams the fatigue strength determining property is also the strain-energy release rate although numerically it is slightly (by approximately 7.5 per cent) smaller than the static G_c. Broadly it may be said that the material has almost the same toughness for static and fatigue loadings.

(12) Since in practice only unnotched beams are loaded in fatigue so that the complication of the stress gradient is avoided, the use of $\sigma^2.c_c$ is very convenient. This value may be determined statically and may then be used in fatigue to predict the critical crack length. If compliance-crack length relationship is available, the compliance at failure may be predicted and impending failure may be anticipated.

(13) The slightly lower fatigue toughness, expressed by $G_{c(fatigue)} = 0.1020$ as against $G_{c(static)} = 0.1100$ lb/in., is attributed to creep.

(14) It is emphasized that the above listed conclusions apply to cement mortar only. Their validity for concrete is yet to be tested.

ACKNOWLEDGEMENTS

This investigation was conducted by the author at the T. & A.M. Dept. of the University of Illinois while on a Sabbatical leave from the Haifa Technion, in 1961/62. It formed part of a broader investigation "Mechanism of Fatigue Failure in Concrete" which was cosponsored by the Division of Highways, State of Illinois and the Bureau of Public Roads, U.S. Dept. of Commerce. The author wishes to thank the sponsors, the Engineering Expt. Stn. of the University of Illinois and in particular Professors T.J.Dolan and C.E. Kesler of the T. & A.M. Department.

REFERENCES

1. Murdock, J.W., and Kesler, C.E., "The Mechanism of Fatigue Failure in Concrete", T.& A.M. Report No. 587, Univ. of Ill., Aug. 1960.

2. Doyle, J.M., Kung, S.H.L., Murdock, J.W. and Kesler, C.E., "Second Progress Report on Fatigue Failure in Concrete", T.& A.M. Report No.601, Univ. of Ill., Sept. 1961.

3. Neal, J.A., Kung, S.H.L. and Kesler, C.E., "Third Progress Report on Fatigue Failure in Concrete", T.& A.M. Report No. 623, Univ. of Ill.

4. Hsu, T.T.C., Slate, F.O., Sturman, G.M. and Winter, G., "Microcracking of Plain Concrete and the Shape of the Stress-Strain Curve", to be shortly published in the ACI Journal.

5. Kaplan, M.F., "Crack Propagation and the Fracture of Concrete", ACI Journal, Proceeding V. 58, No. 5, Nov. 1961, pp. 591-610.

6. Irwin, G.R. and Kies, J.A., "Fracturing and Fracture Dynamics", Welding Journal, V. 31, 1952, p. 95-S.

7. Glucklich, J., "On the Compression Failure of Plain Concrete", T.& A.M. Report No. 215, Univ. of Ill., March 1962.

8. Bingham, E.C. and Reiner, M., "Rheological Properties of Cement and Cement-Mortar-Stone", Physics, V.4, March 1933, pp. 88-96.

9. Blakey, F.A. and Beresford, F.D., "Tensile Strains in Concrete Parts 1 and 2", Report No. C2.2-1 and No. C2.2-2, Division of Building Research Commonwealth Scientific and Industrial Research Organization (Australia) 1953 and 1955.

10. Winne, D.H., and Wundt, B.M., "Application of the Griffith-Irwin Theory of Crack Propagation to the Bursting Behaviour of Discs Including Analytical and Experimental Studies", Trans. ASME, V. 80, 1958, pp. 1643-1655.

11. Glucklich, J., "Static Fatigue in Concrete", Rheologia Acta, Band 1, No. 4/6, 1961, pp. 356-361 (Darmstadt).

12. Hilsdorf, H. and Kesler, C.E. "The Behaviour of Concrete in Flexure Under Varying Repeated Loads", T. & A.M. Report No. 172, Univ. of Ill. Aug. 1960.

13. Murdock, J.W., and Kesler, C.E., "Effect of Range of Stress on Fatigue Strength of Plain Concrete Beams", ACI Journal Proceedings. V. 55, No. 2, Aug. 1958, pp. 221-231.

14. Glucklich, J., "Fracture of Plain Concrete", Proceed. ASCE, V. 89, No. EM 6, Dec. 1963, pp. 127-138.

TABLE 1

EXAMPLE OF FATIGUE DATA OF AN UNNOTCHED BEAM

SPECIMEN NO.: FG-49 DATE:Mar. 23, 1962. MACHINE No.:2

DYNAMOMETER CONST = 0.748 DEFORMETER CONST = 0.3056

TEST STRESSES: 670 psi to 50 psi INDICATOR: 896 to 67

Cycles	Dynamometer max	Dynamometer min	Deformeter max	Deformeter min	Δ_{max}	Δ_{min}	$\frac{\epsilon_{max}\ \epsilon_{min}\ \epsilon_{max}-\epsilon_{min}}{(10^{-6}\text{in./in.})}$	$\text{Dyn}_{max} - \text{Dyn}_{min}$	$\sigma_{max} - \sigma_{min}$ (psi)	Compliance L_ϵ $(10^{-6}\ \frac{\text{in.}^2}{\text{lb}})$	$C^{(6)}$ (in.)
No.Load	860	860	1490	1490							
	896	67									
Zero	1756	927									
0	1760	925	770	1400	720	90	220 27.5 192.5	835	624	0.308	0.185
500	1755		770								
Reset	1760	925	765	1390	725	100	222 30.5 192.0	835	624	0.308	0.185
2500	1750		755								
Reset	1760	930	740	1370	750	120	229 36.6 192.0	830	620	0.310	0.200
10,000	1750		730								
Reset	1760	940	720	1350	770	140	235 42.7 192.0	820	613	0.313	0.230
52,000	1760	935	690	1320	800	170	244 51.0 193.0	825	616.5	0.313	0.230
100,400	F A I L U R E										

(6) From compliance vs crack-length in Fig. 20

TABLE 2

	(1) Mean f'_r from Full beams	(2) Mean f'_r from all ¼ beams	(3) Mean f'_r from all beams and "halves"	(4) Mean f'_r from "halves of same beams of col.(1)	(5) Corrected mean f'_r from full beams	(6) f'_c 6 x 12 in. cyl.
	psi	psi	psi	psi	psi	psi
Unnotched-beams Series A	760	790	788	-	-	5160
Unnotched-beams Series B	-	968	968	-	-	-
Notched-beams Series C,D & E	373	880	-	887	370	5740

column (5) was derived from: (5) = $\frac{(1)}{(4)}$ x (2)

TABLE 3

EVALUATION OF $\sigma_{max} \cdot C_c$ AND $\sigma^2_{max} \cdot C_c$ FOR FATIGUE BEAMS

Specimen No.	Type of Specimen	Series	σ_{max} (psi)	C_c (in.) (From Graphs)	$\sigma_{max} \cdot C_c$ (lb/in.)	$\sigma_{max}^2 \cdot C_c$ ($lb^2/in.^3$)
FG 38	Unnotched beams	A	600	0.280	168	101,000
FG 39		"	563	0.295	166	93,500
FG 43		"	650	0.260	169	111,000
FG 49		"	670	0.243	163	109,000
FG 50		"	670	0.270	181	121,500
FG 51		"	630	0.245	155	101,000
FG 52		"	650	0.250	163	105,500
FG 53		"	620	0.270	168	104,000
FG 54		"	620	0.250	155	96,200
FG 55		"	703	0.210	148	104,000
FG 59		"	688	0.265	182	125,500
FG 60		"	704	0.210	148	104,200
FG 61		"	690	0.268	185	127,500
FG 64		"	570	0.320	182	104,000
FG 65		"	625	0.355	222 x	138,500 x
FG 66		"	670	0.250	168	112,500
			mean		167	110,800
			coeff.of variation		6.95%	11.61%
FGW 2	Notched Beams	C	290	1.280	372	110,500
FGW 3		"	298	1.165	347	103,500
FGW 4		"	296	1.150	341	101,000
FGW 5		"	310	1.100	341	105,500
FGW 6		"	300	1.135	341	102,300
FGW 8		"	325	1.040	338	111,000
FGW 9		"	335	1.050	352	117,500
FGW 10		"	310	1.115	346	97,800
FGW 11		"	330	1.080	356	116,500
FGW 12		"	280	1.020	286 x	80,000 x
FGW 14		"	290	1.160	336	97,500
FGW 15		"	340	1.000	340	115,000
FGW 18		"	330	1.010	334	110,000
FGW 55		"	300	1.150	345	103,500
			mean		345	105,000
			coeff. of variation		2.69%	6.42%

x Not included in coeff. of variation.

(continued)

TABLE 3 -concluded-

EVALUATION OF $\sigma_{max}.C_c$ AND $\sigma^2_{max}.C_c$ FOR FATIGUE BEAMS

Specimen No.	Type of Specimen	Series	σ_{max} (psi)	C_c (in.) (From Graphs)	$\sigma_{max}.C_c$ (lb/in.)	$\sigma^2_{max}.C_c$ (lb^2/in.^{3})
FGW 25	Notched Beams	D	300	1.230	368	111,000
FGW 26		"	325	1.090	354	115,000
FGW 27		"	315	1.155	363	114,500
FGW 32		"	290	1.195	346	100,500
FGW 33		"	300	1.180	354	106,200
FGW 34		"	280	1.295	362	103,000
FGW 35		"	330	1.070	353	116,000
FGW 38		"	270	1.370	370	100,000
FGW 39		"	280	1.290	361	101,500
FGW 40		"	290	1.190	345	100,000
FGW 41		"	300	1.180	354	106,200
FGW 44		"	280	1.280	358	100,700
FGW 49		"	295	1.240	365	108,000
			mean		358	106,500
			coeff. of variation		1.97%	5.34%
FGW 45	Notched Beams	E	340	0.960	327	111,000
FGW 46		"	300	1.260	378	113,500
FGW 47		"	320	1.075	344	110,000
FGW 53		"	310	1.190	369	114,000
FGW 54		"	270	1.320	356	96,500
FGW 62		"	260	1.490	387	101,000
FGW 64		"	280	1.285	360	101,000
FGW 65		"	280	1.290	361	101,300
FGW 66		"	270	1.360	367	99,500
			mean		361	105,500
			coeff.of variation		4.05%	6.00%

TABLE 4

EVALUATION OF $\sigma_{St}.C_c$ AND $\sigma^2_{St}.C_c$ FOR STATIC BEAMS (SERIES F)

Specimen No.	Type of Specimen	σ_{St} (psi) from Figs. 17,18	L_e (10^{-6} in^2/lb) From Fig. 17	L_e (10^{-5} in^3/lb) From Fig. 18	C_c (in.) From Fig. 20	$\sigma_{St} \times C_c$ (lb/in.)	$\sigma^2_{St} \times C_c$ (lb^2/in.^{3})
FG 19	Unnotched beams	764	0.314		0.22	168	128,000
FG 22		787	0.307		0.18	142	111,500
FG 33		710	0.317		0.24	170	121,000
FG 37		765	0.314		0.22	168	129,000
FG 45		792	0.307		0.18	143	113,000
FG 46		740	0.314		0.22	163	121,000
	Means	759			0.21	159	121,000
FGW 7	Notched beams	325		0.277	0.99	322	104,800
FGW 13		340		0.259	0.93	316	107,500
FGW 16		385		0.234	0.83	320	123,000
FGW 36		340		0.259	0.93	316	107,500
FGW 42		340		0.279	0.99	336	114,500
FGW 48		330		0.273	0.97	320	106,000
FGW 61		345		0.275	0.98	338	116,500
	Means	343			0.946	324	111,500

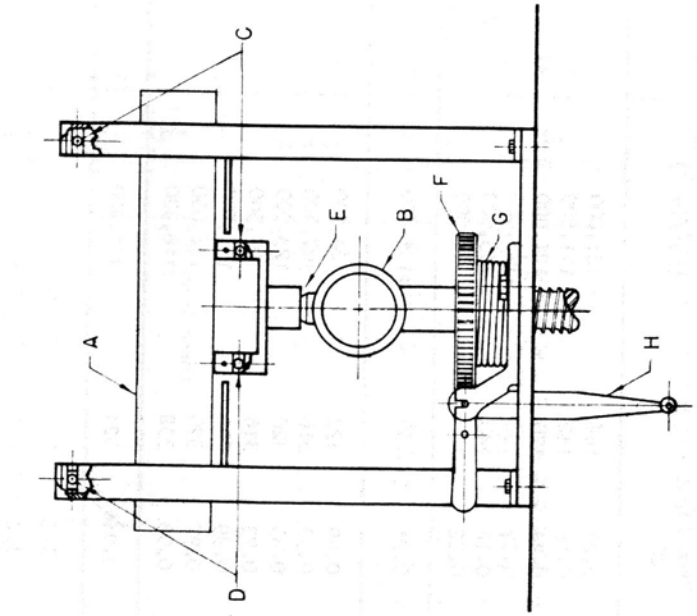

Fig. 2 Schematic Diagram of Bending Static Machine

A - Specimen
B - Dynamometer
C - Roller Supports
D - Ball Supports
E - Swivel Joint
F - Gear
G - Tension Spring
H - Crank

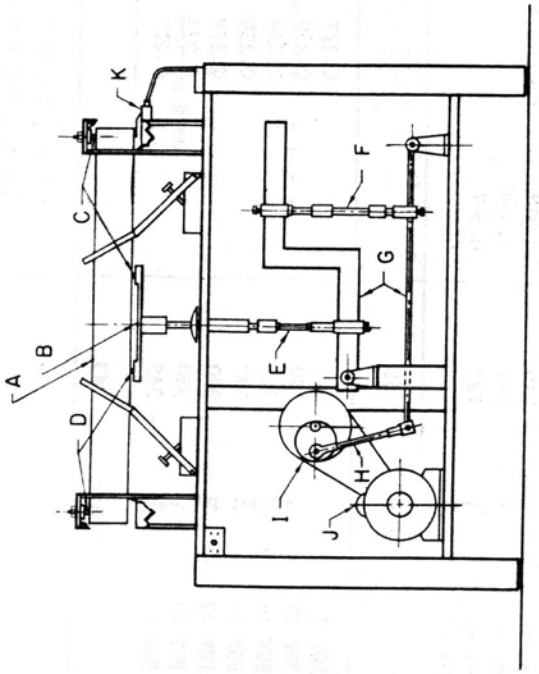

Fig. 1 Schematic Diagram of Bending Fatigue Machine

A - Specimen
B - Dynamometer
C - Roller Supports
D - Ball Supports
E - Connecting Rod
F - Adjustable Connecting Rod
G - Load Levers
H - Connecting Rod
I - Eccentric
J - Motor
K - Automatic Cut-off Switch

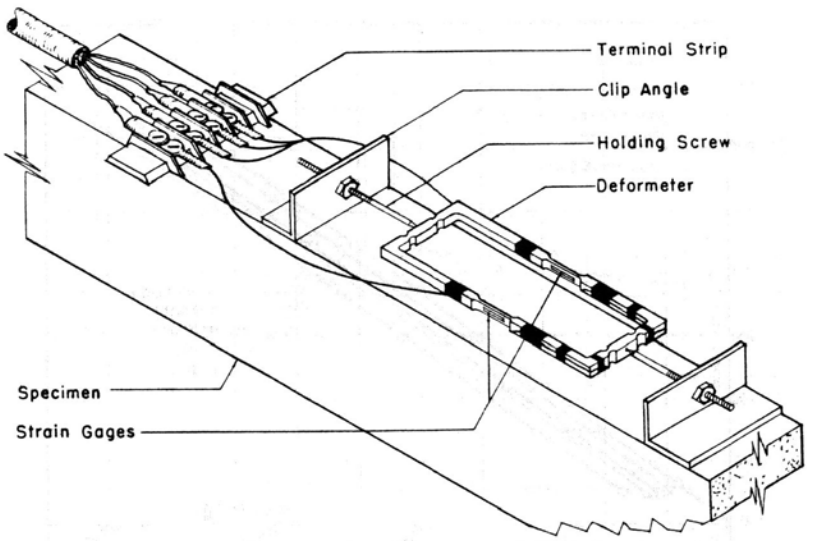

Fig. 3 Schematic Detail of Deformeter on A Test Specimen

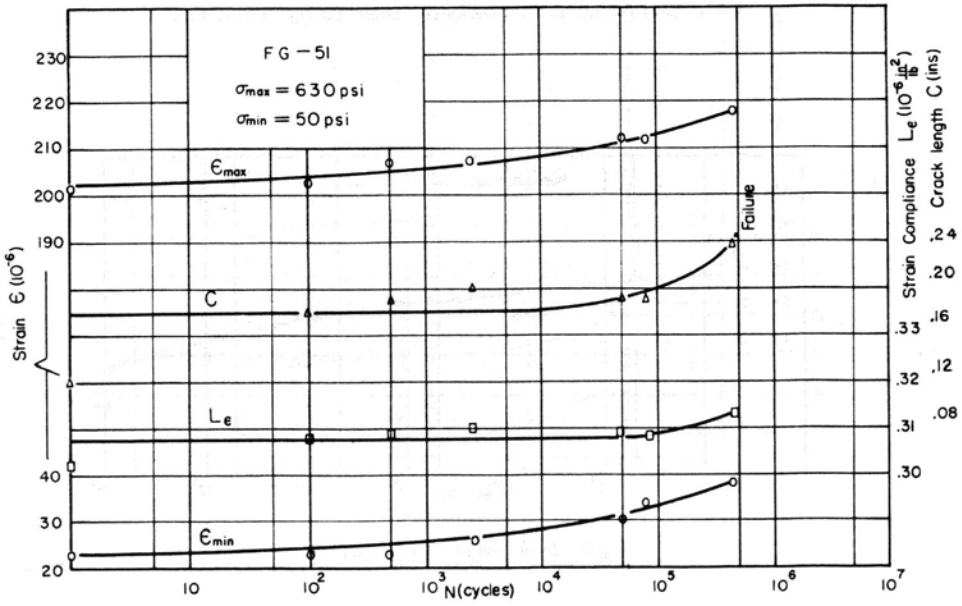

Fig. 4 Unnotched Beam in Fatigue. Series A

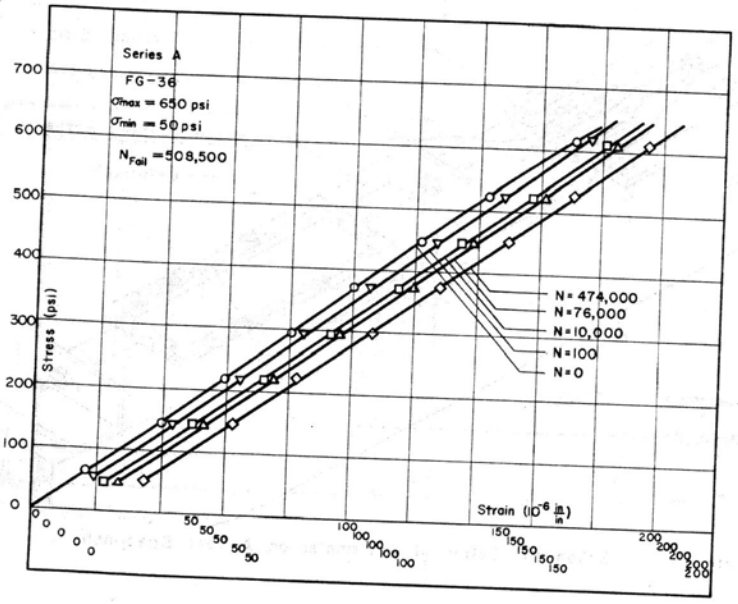

Fig. 5 Stress-Strain of an Unnotched Beam During Fatigue Life

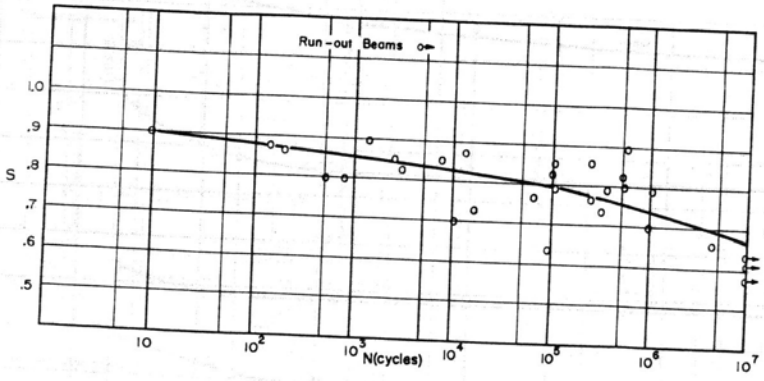

Fig. 6 S–N Curve for Series A

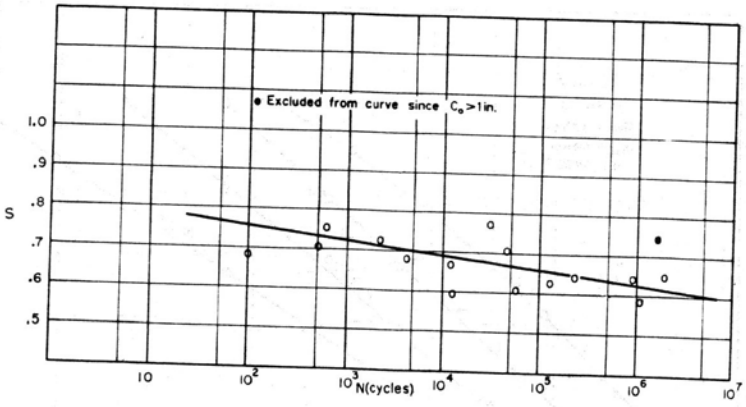

Fig. 7 S–N Curve for Series B

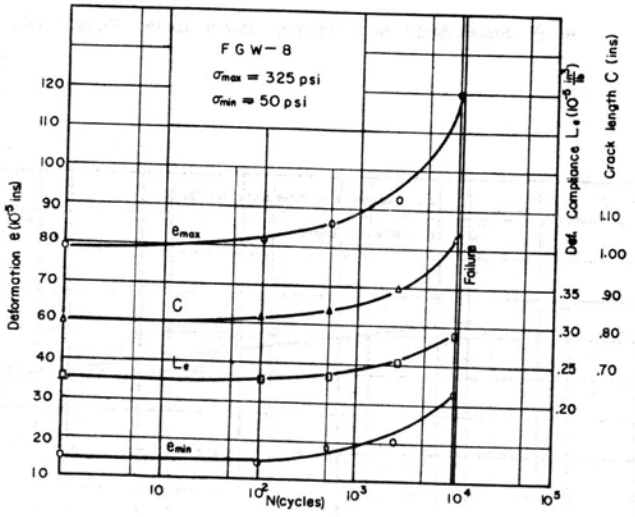

Fig. 8 Notched Beam in Fatigue. Series C

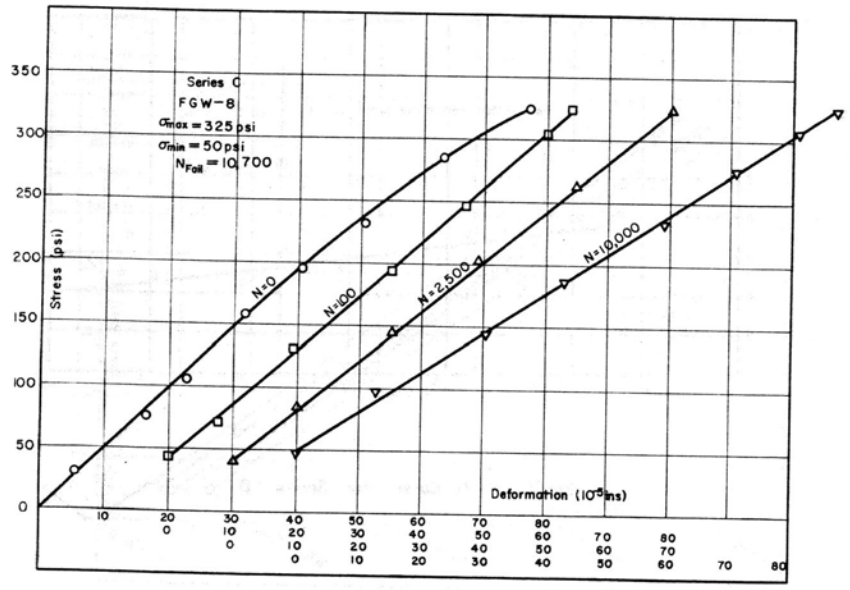

Fig. 9 Stress-Strain of a Notched Beam During Fatigue Life

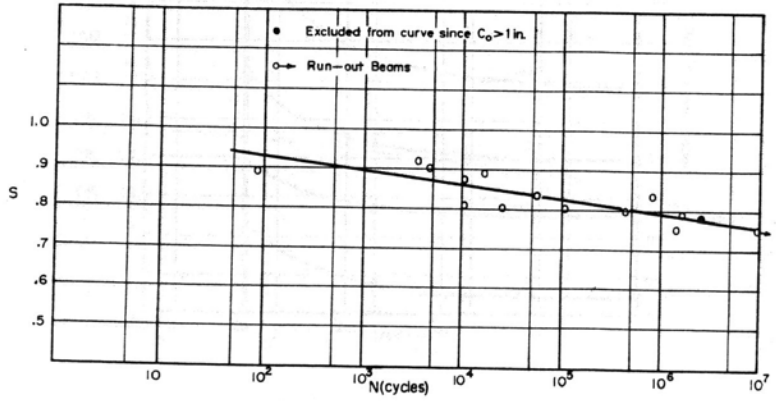

Fig. 10 S—N Curve for Series C

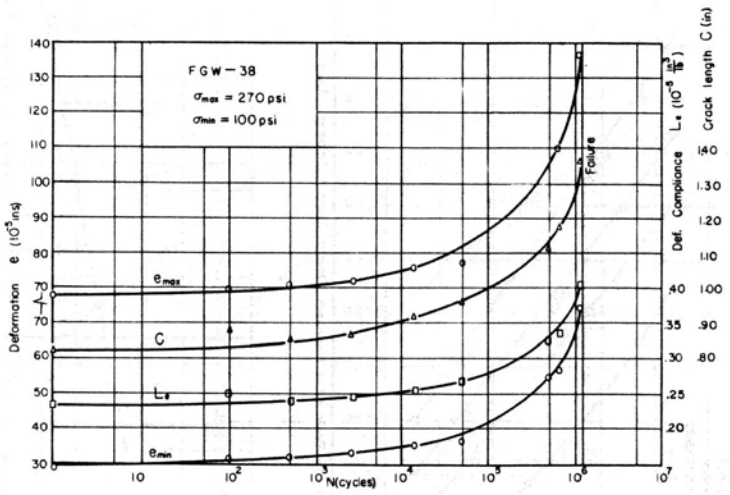

Fig. 11 Notched Beam in Fatigue. Series D

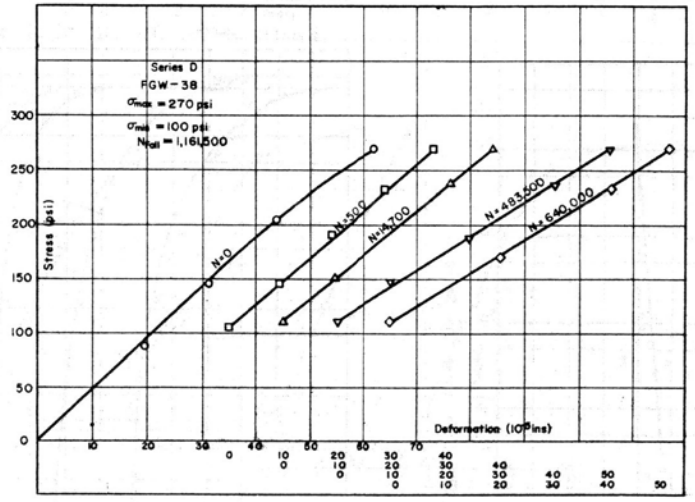

Fig. 12 Stress-Strain of a Notched Beam During Fatigue Life

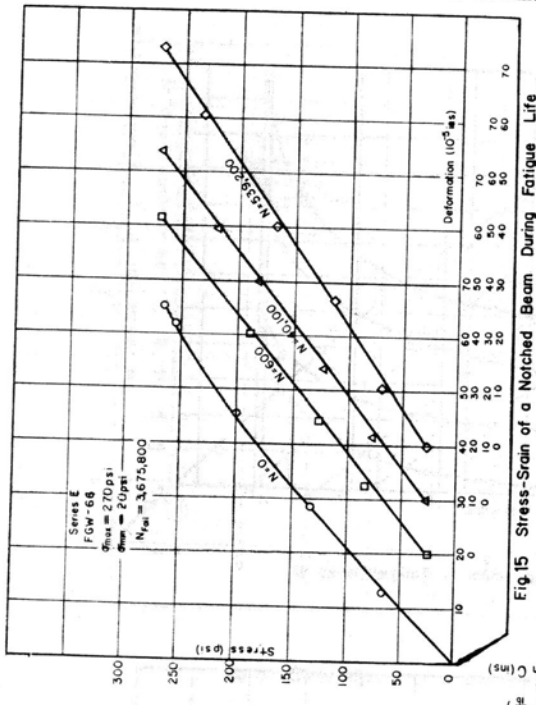

Fig.15 Stress-Strain of a Notched Beam During Fatigue Life

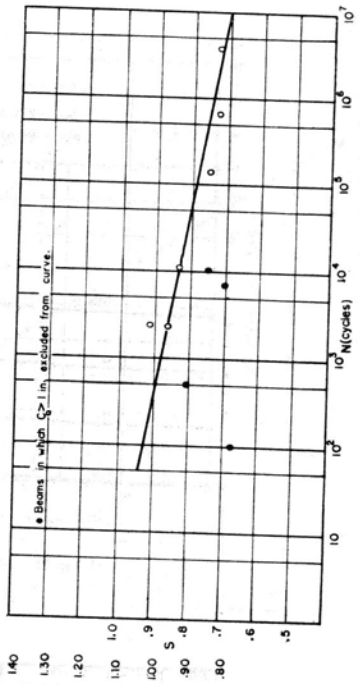

Fig.16 S-N Curve for Series E

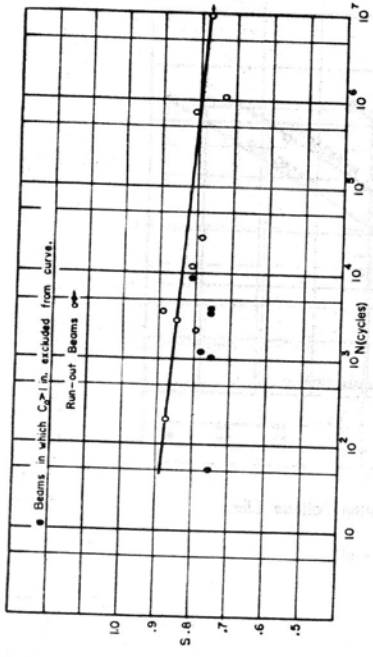

Fig.13 S-N Curve for Series D

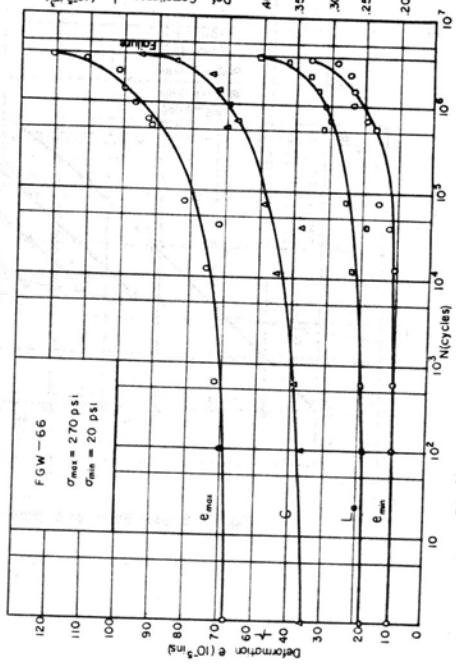

Fig.14 Notched Beam in Fatigue. Series E

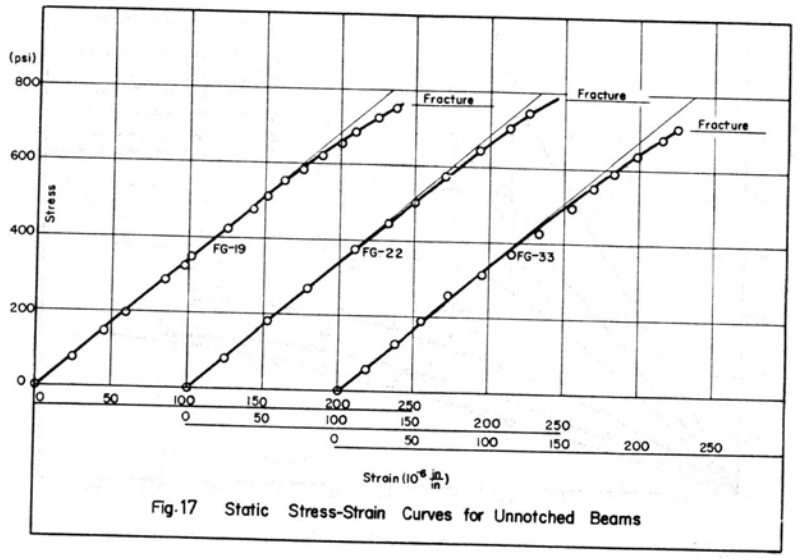

Fig.17 Static Stress-Strain Curves for Unnotched Beams

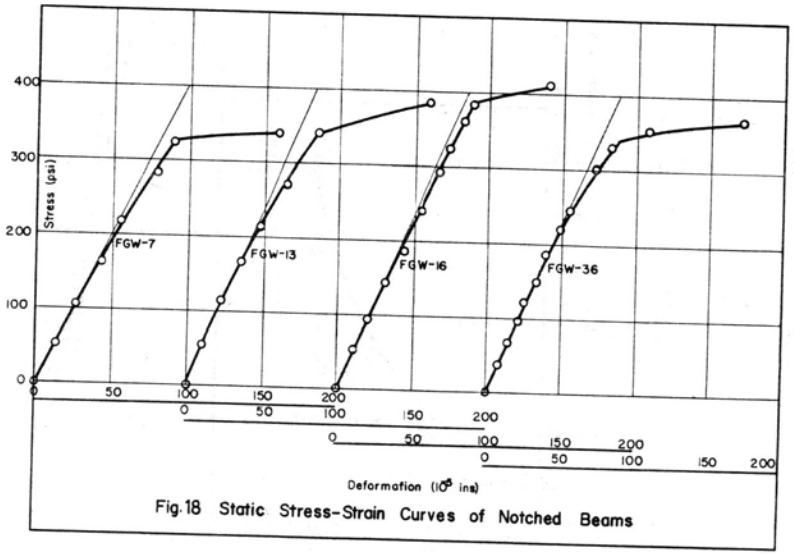

Fig.18 Static Stress-Strain Curves of Notched Beams

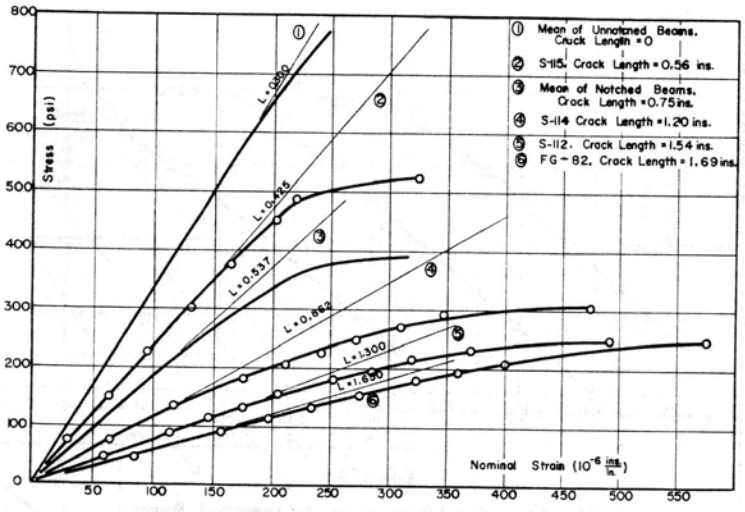

Fig. 19 Stress-Strain Curves of Beams with Natural Cracks of Varying Depths

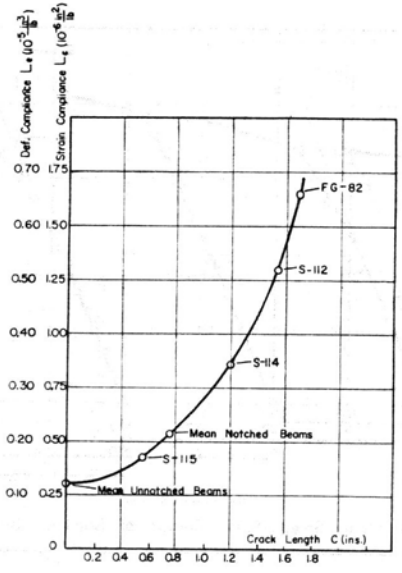

Fig. 20 Dependence of Compliance on Crack Length

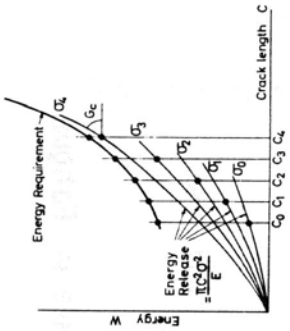

Fig. 23 The Forced Growth of a Crack

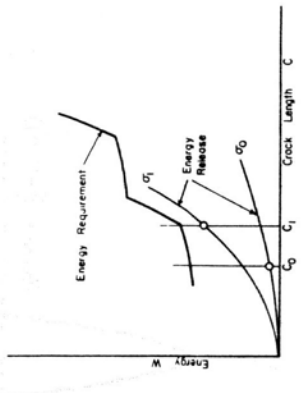

Fig. 24 A Crack Progressing in a Bi-phase Material

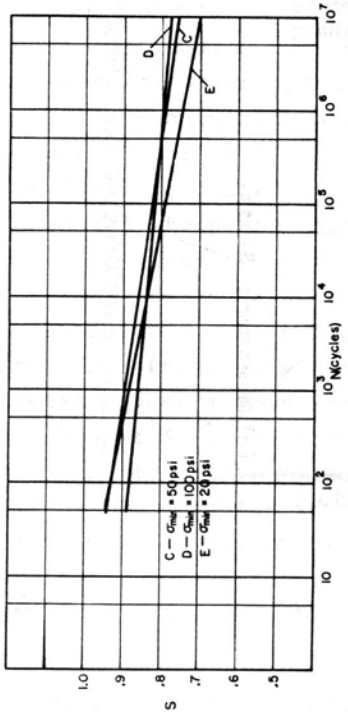

Fig. 21 Effect of Range of Stress on S-N Curves. Results of Series C, D and E Superposed.

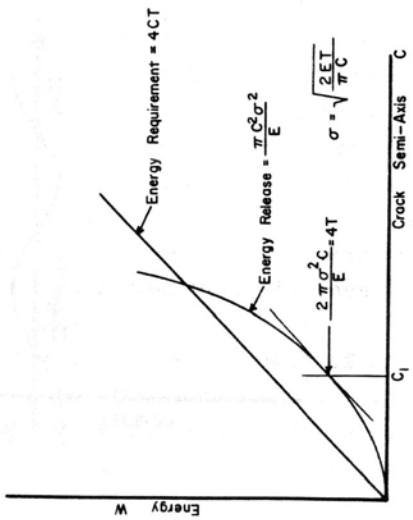

Fig. 22 The Griffith Case

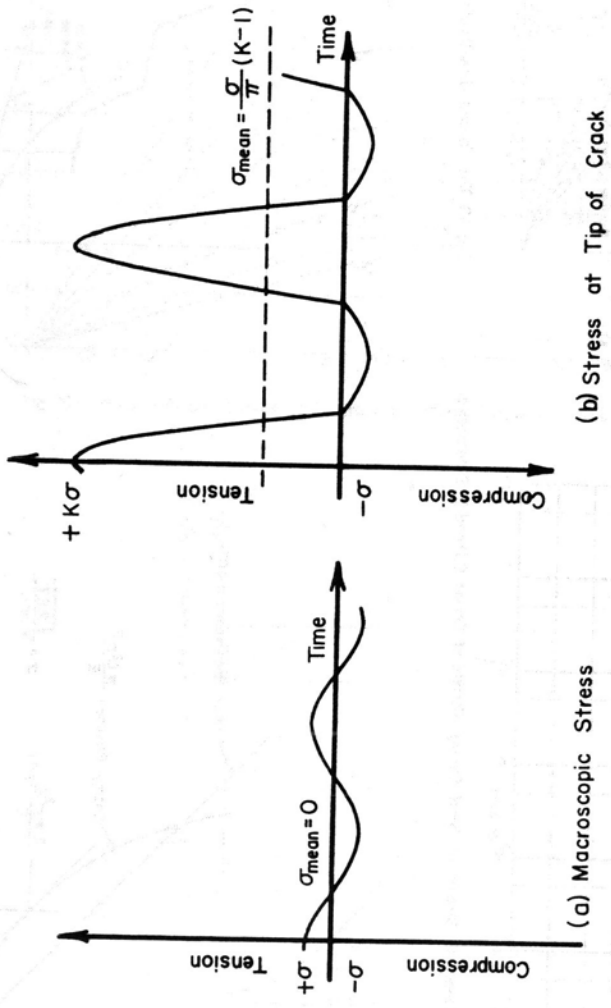

Fig. 25 Macroscopic and Microscopic Stresses in Fatigue

C-20

Concerning the Method of Evaluating the Strength of an Oriented Solid Polymer

G.M. Bartenev* and I.V. Rasumovskaya*

ABSTRACT

1. To build up a fully oriented structure is one of the most effective ways of producing high-strength amorphous solid polymers. In their works Hsiao and his associates proposed statistical methods for calculating the strength of oriented polymers, which are of great practical importance. In our works we made an attempt to evaluate the strength of a fully oriented polymer at stretching by a somewhat different approach using the equation for the time dependence of strength, which was proposed by one of the authors in 1955.

2. Calculations were made for two models of an amorphous solid polymer: a classical model of a polymer with random structural of chains and a model of a solid polymer with a "piled up" structural chains. The evaluations have shown that the coefficient of strengthening (ratio between the strength of a fully oriented polymer and that of a non-oriented polymer) is dependent on the molecular and supramolecular polymeric structures (mean length of macromolecule segment, distance between segments, mean sizes of "piles", etc.).

3. It is shown that the increase in the strength of a solid polymer with orientation is explained primarily not by changes in molecular interaction, but by changes in the average number of chemical bonds broken per unit surface area of the specimen cross-section. The coefficient of strengthening can reach big values, in the order of 10 and even greater.

* Department of the Solid State Physics of the Lenin State Teachers' Training University, Moscow